Materials Science and Engineering C 29 (2009) 2471–2477

Contents lists available at ScienceDirect

Materials Science and Engineering C

journal homepage: www.elsevier.com/locate/msec

Analysis of the fatigue behaviour characterized by stiffness and permanent deformation for different distal volar radius compression plates

M. Schüller [a,*], H. Drobetz [b], H. Redl [c], E.K. Tschegg [a]

[a] Material Science Laboratory, Institute for Building Construction and Technology, University of Technology, Karlsplatz 13, A-1040 Vienna, Austria
[b] Orthopaedic Department, Mackay Base Hospital, 439 Bridge Road, Mackay, QLD, Australia
[c] Ludwig Boltzmann Institute for Experimental and Clinical Traumatology, A-1200 Vienna, Austria

ARTICLE INFO

Article history:
Received 18 November 2008
Received in revised form 11 February 2009
Accepted 14 July 2009
Available online 25 July 2009

Keywords:
Radius implant
Distal volar compression
Fatigue
Permanent deformation
Stiffness

ABSTRACT

Fractures of the distal radius are with 10% the most frequent fractures of the human skeleton. In order to stabilize the fracture which is essential for succesful bone-healing, distal volar compression using dorsal compression plates is often used. Among the most important, but until now sparsely investigated criteria for implant-quality is the fatigue behaviour of the system of radius and stabilizing implant. Several types of implants were tested in combination with synthetic bones in the fatigue regime. The fatigue behaviour of samples was characterized using the parameters stiffness, tilting angle and reduction of the fracture gap which can be expressed by the permanent deformation of the system. The study of the evolution of these properties allows an interpretation of the mechanisms governing fatigue. Thus, a comparison of different implant types was obtained. Results show that the geometry of the implant as well as the positioning and type of the used screws has a profound effect on the characteristics of the system.

1. Introduction

In order to provide means for selecting an implant for the treatment of bone-fractures, it is important to characterize relevant properties of the implant. One approach is to study the properties of the implant [1,2] and supported bone [3] itself. This paper takes another approach and concentrates on the whole system of bone and implant. The same approach was also taken by some earlier studies [12,13,15]. It comes with the drawback of higher complexity for the measurements; therefore some cutbacks have to be done. Measurements on cadaveric bones [4,20] show, that there exists a high sample to sample variation due to variations in specimen geometry and material. For this reason, synthetic bones from Sawbones® were used in this study. Furthermore, the physiological situation of the system will have an influence on the results. However, the task of this study is not to give exact mechanical values of the bone–implant system which should be applicable to clinical praxis, but to show that the testing technique is sensitive to the differences between different systems. Some studies focused on the mechanical properties of the bone–implant interface in the cortical bone [11], but don't include fatigue behaviour and permanent deformation.

This study concentrates on the determination of mechanical properties of fractured radius-bones of AO-type 23C2 treated with several distal volar locking plates in the fatigue regime. We want to show that the testing setup is representative for the clinical scenario which means that it leads to the same failure modes as observed in the clinical praxis. Furthermore, the study points out differences in the fatigue behaviour of different implants, the timing and localisation of failure and explains the results. With the help of sophisticated calculation routines which were developed in a preceding study [5], the parameters' permanent deformation and stiffness of the whole system can be depicted for every cycle of loading. This allows the comparison of the evolution of these parameters over the fatigue sequence. The interface with medical parameters is obtained by calculation of the tilting angle between distal epiphysis and bone shaft in the sagittal plane.

After fatigue testing, the distal metaphyseal fragment is subjected to failure test in order to obtain ultimate load and fracture energy.

2. Materials and methods

The used bones are of the type "Sawbones® [19] 1018 Large Left Radius". The synthetic bones have the advantages of small spread in properties (discussed in Section 1) and are easy to store and handle. The synthetic bones are made of solid foam. A comparison of material properties of the used synthetic bone material with cadaveric bone material was conducted in a study by Liska et al. [24]. The implants were of 4 different designs from 3 manufacturers Hofer®, Stryker® and Synthes®. Fig. 1 shows the different implants. The implant from Stryker® is made of Grade 5 titanium (Ti6Al4V) and anodized to reduce tissue adhesion. The Hofer® and Synthes®-implants are made from pure titan (ISO 5832-2).

* Corresponding author.
E-mail address: michael.schueller@gmx.at (M. Schüller).

0928-4931/$ – see front matter © 2009 Elsevier B.V. All rights reserved.
doi:10.1016/j.msec.2009.07.013

Fig. 1. Sample-types; two implants of the same type with different screw-realisation were tested in case of Hofer®.

In case of the Hofer® implant, a variation of screw-type was investigated, the green screws are locking screws of spongiosa type and the violet ones are corticalis-locking screws. The difference between these screw types is the design of the thread. The spongiosa-screw shows a more coarse thread than the corticalis screw. The implants were fixed on the bones and the fracture incorporating a transversal as well as a sagittal fracture was introduced into the samples using a saw. The bones were cut about 15 cm proximal of the transversal fracture gap and fixed into sample carriers. The material testing machine for fatigue testing is a servohydraulic Schenck Hydropuls PSA and the load to failure tests were carried out using a mechanical 100 kN material testing machine from Schenck (more details in [5,10]).

The sample fixtures for fatigue testing must guarantee realistic loading of the specimen. Therefore, a cast of the distal joint-plane was created using bone cement [23] for the distal side, and the bone shaft was fixed (encastre-type) to the testing machine using a fitting of the sample carrier. The testing program in the fatigue regime shall represent the first 6 weeks of bearing after implantation. According to a preceding study [4], a sinodial variation of force with amplitude of 800 N and 2000 cycles with a frequency of 1 Hz is a conservative scenario for the axial loads the radius-bone is subjected to during the 6 weeks following implantation. Due to the measurement technique, the system can't be totally unloaded since this would lead to problems with specimen alignment. Over the whole fatigue sequence, the actual force and displacements on different positions were measured using a load-cell and inductive displacement sensors (LVDT) as well as videoextentiometry. The schematic test-setup is shown in Fig. 2. The light grey arrows indicate forces acting on the specimen in axial direction. Dark grey arrows show the position of displacement sensors. In the case of screws and proximal implant, the displacements were measured using videoextentiometry.

2.1. Sample size

Three samples were tested for every implant. After fatigue testing, a load to failure test was conducted for the distal part of the system to test the stability of the distal fracture system.

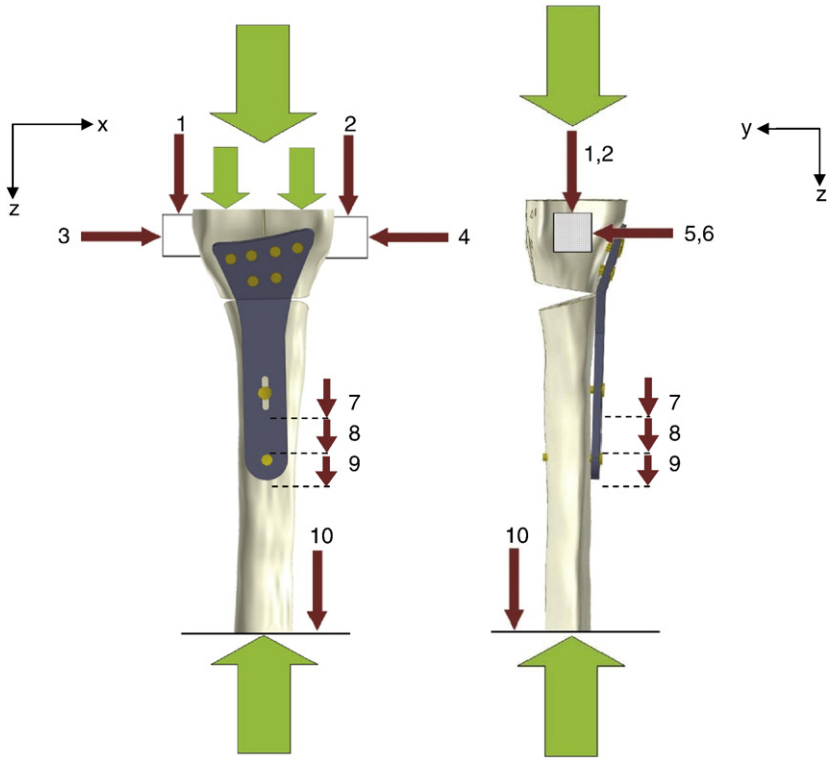

Fig. 2. Position of sample and sensors, the light grey arrows show axial forces, the dark grey arrows show the location of displacement sensors and extentiometer.

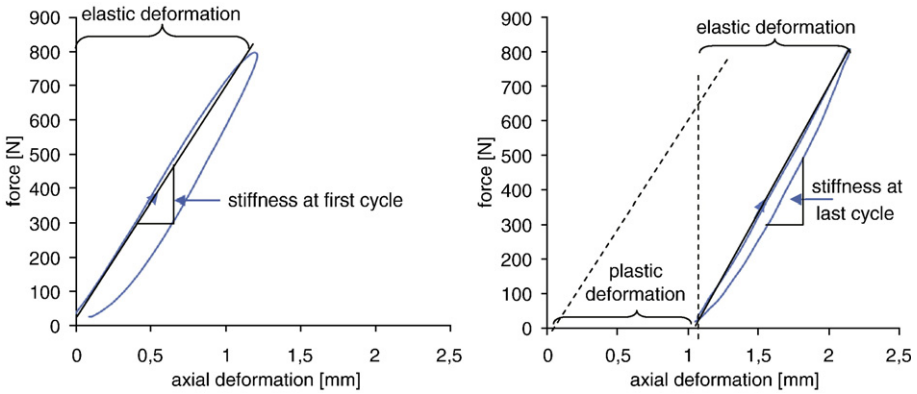

Fig. 3. Axial deformation during the first (left) and last (right) cycles of the fatigue sequence. The parameters' stiffness (slope of the force–displacement curve), elastic and permanent deformation are shown.

3. Presentation and evaluation of data

The recorded values of displacement and force were used to calculate characteristic values of the implant like stiffness, elastic deformation, plastic deformation, tilting angle for the two fracture systems sagittal fracture and transversal fracture. The calculation routines are shortly outlined, for further information see Ref. [5].

Fig. 3 emphasizes the parameters stiffness, plastic and elastic deformation. It shows the axial displacement as a function of load, the arrow marks the direction of loading, as can be seen, the unloading sequence show slightly higher displacements. The area enclosed by the curve is the dissipated energy which leads to plastic deformation of bone and implant and heating up of the system. Another parameter important for characterization of the system in respect to medical criteria is the tilting angle of the system. The displacement of the distal fracture-system with respect to the bone shaft leads to a tilt of the system (the axis of rotation is the implant at the position of the transversal fracture gap). The tilting angle can be calculated and related to the medical allowable. Thus a criterion for implant failure is obtained. According to [6], a permanent tilt of more than 5° induces restrictions in movement of the joint.

The load to failure test yields an ultimate load of the distal system. With the measurement of axial displacement, a calculation of fracture energy is possible. This energy is absorbed by the system during loading. Some part of the energy is stored elastically and released after breaking, the other part is absorbed by the system during loading in the form of permanent deformation, crack initiation and formation and heat. A relatively higher fracture energy means the system can absorb more energy before failure.

4. Results

Table 1 lists the obtained mean values and standard deviations of the discussed parameters. Since a serious statistic is not possible with a population size of 3 samples, the values of standard deviation should be used as a measure for sample spread when comparing different systems, but not as an absolute value.

Fig. 4 shows the evolution of axial stiffness over the fatigue sequence.

The stiffness of all implants shows a steep increase at lower cycles. For most of the implants, this increase slows down for higher cycles. The implants HOF_G and SYN_3.5 show a decrease of stiffness at a higher cycle count. The change in stiffness after the initial increasing period is, however, lower than 10%, except for the Stryker® (STR) implant which shows a non-uniform increase of stiffness over the whole fatigue period.

Fig. 5 shows the evolution of axial permanent deformation and the resulting tilting angle between distal and proximal fracture fragments.

Different implants show a remarkable difference in axial permanent deformation. All samples show a steep increase of permanent deformation during the initial 250 cycles. After 1500 cycles, samples with implants Stryker® and Synthes® 3.5 show a relatively greater increase of permanent deformation than the other samples. Especially the implant Stryker® shows high deformation. The implants HOFER_G and HOFER_R with different locking screws (see Section 2) show

Table 1
Mean values and standard deviations of stiffness, permanent deformation for the transversal (axial) and sagittal fracture system as well as permanent tilting angle for the implants under fatigue loading.

Implant	SYN_3.5	SYN_2.4	STR	HOF_R	HOF_G
Axial stiffness [N/mm]					
First cycle	531 ± 32	644 ± 15	556 ± 94	839 ± 250	708 ± 123
Last cycle	535 ± 93	652 ± 17	613 ± 162	865 ± 201	698 ± 120
Axial permanent deformation [mm]					
Last cycle	0.82 ± 0.16	0.47 ± 1.97	1.71 ± 1.26	0.34 ± 0.06	0.69 ± 0.37
Permanent tilting angle [°]					
Last cycle	3.09 ± 0.61	1.76 ± 0.74	6.4 ± 4.7	1.3 ± 0.2	2.6 ± 1.4
Stiffness [N/mm]					
First cycle	5298 ± 2437	3999 ± 1194	2984 ± 323	3802 ± 761	4100 ± 1009
Last cycle	4061 ± 667	3920 ± 1293	3048 ± 392	3865 ± 768	2864 ± 1200
Plastic deformation [mm]					
Last cycle	0.002 ± 0.06	0.04 ± 0.05	0.13 ± 0.03	0.03 ± 0.003	0.56 ± 0.41

The results are shown for the beginning and end of the fatigue sequence.

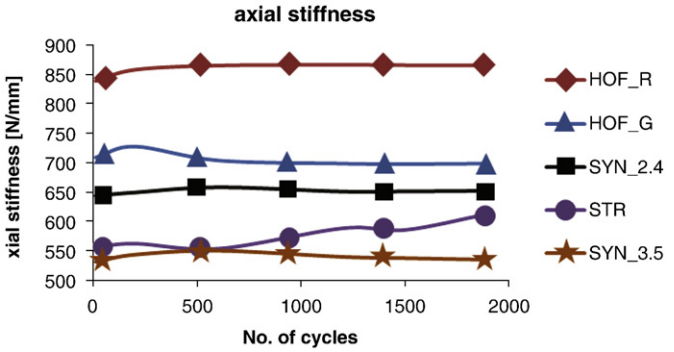

Fig. 4. Evolution of axial stiffness over the fatigue sequence of 2000 cycles. The implants are labelled in the following way: HOF_R is the Hofer®-implant incorporating 6 corticalis-locking screws at the most distal positions, HOF_G abbreviates the Hofer®-implant with 4 corticalis and 2 spongiosa locking screws at the distal positions. SYN_2.4 and SYN_3.5 define the Synthes® implants with 2.4 mm and 3.5 mm screws resp. STR states fort the Stryker® implant.

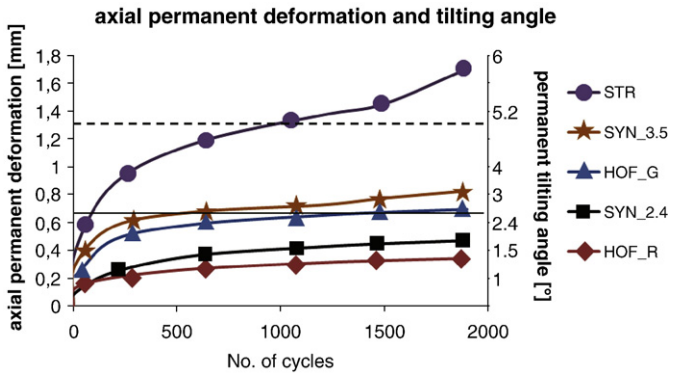

Fig. 5. Evolution of axial permanent deformation over the fatigue sequence of 2000 cycles. The implants are labelled in the following way: HOF_R is the Hofer®-implant incorporating 6 corticalis-locking screws at the most distal positions, HOF_G abbreviates the Hofer®-implant with 4 corticalis and 2 spongiosa locking screws at the distal positions. SYN_2.4 and SYN_3.5 define the Synthes® implants with 2.4 mm and 3.5 mm screws resp. STR states for the Stryker® implant. The secondary axis measures the permanent tilting angle. The tilting angles 2.5° and 5° are marked as horizontal lines. Further explanations are given in the text.

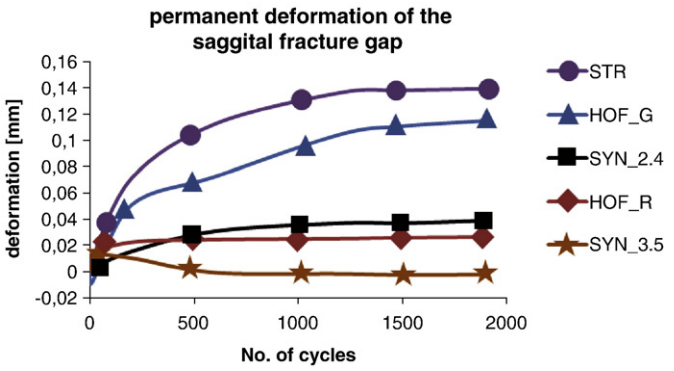

Fig. 7. Evolution of permanent deformation of the sagittal fracture gap. This deformation results in a widening of the sagittal fracture gap. As can be seen, the absolute deformation is low. Stryker® and Hofer® implants with standard and locking screws show the greatest deformation.

different behaviour of permanent deformation. The variation with 5 corticalis-locking screws on the distal side shows just half of the axial permanent deformation at the end of the fatigue sequence when compared with the variant with corticalis and spongiosa locking screws. The permanent (dorsal) tilting angle between distal and proximal fragment depends on the axial permanent deformation. Fig. 5 shows the permanent tilting angle on the secondary (right) axis. Horizontal lines mark the 2.5° and 5° permanent tilting angles. These angles will be use for further evaluation of the stabilizing properties (see Section 5).

The sagittal fracture fragments are stabilized through the distal screws of the implants. Analogously to the transversal fracture, stiffness and permanent deformation of this fracture system can be calculated from the measurements.

Fig. 6 shows the stiffness of the sagittal fracture system. The most interesting fact is that the absolute values are about one order of magnitude higher than in the case of the axial stiffness at the transversal fracture system. Moreover, most implants show a decrease in stiffness. The implant HOF_G shows a decrease of stiffness after 500 cycles and ends up with the lowest stiffness after the fatigue period. The implant SYN_3.5 starts with the highest stiffness of all implants which, however, decreases to roughly the stiffness of HOF_R and SYN_2.4 after the first 500 cycles. Further details will be discussed in Section 5.

Fig. 7 depicts the evolution of permanent deformation of the sagittal fracture system. Most implants show a negligible permanent deformation, with the exception of the Stryker® and HOF_G implants.

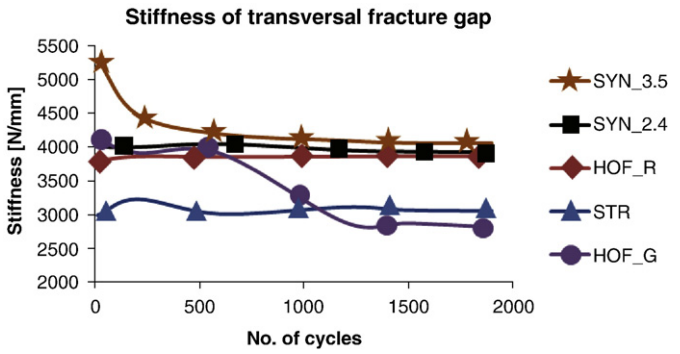

Fig. 6. Stiffness of sagittal fracture gap over the fatigue sequence. All implants show a decrease in stiffness, the highest decrease occurs for the SYN_3.5 implant. The HOF_G implant shows a not uniform decrease.

In addition to the fatigue test of the whole system of bone and implant, a load to failure test of the distal fracture system and the implant was conducted.

Fig. 8 shows the maximum force reached during the load to failure experiment. At this force, some implants showed breaking of screws (SYN_2.4), breaking of the threads of locking screws in the implant (HOF_G, HOF_R), or failure of the bone material supporting the screws (Stryker, SYN_3.5).

Fig. 9 depicts the deformation energy which was dissipated through the loading until failure. It is a measure for the energy which can be absorbed by the system before failure.

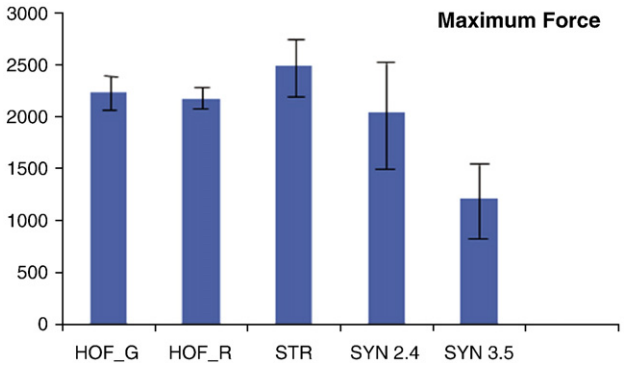

Fig. 8. Maximum force reached at the load to failure test. The black bars show the standard deviation of the mean value which is depicted through the light grey bars.

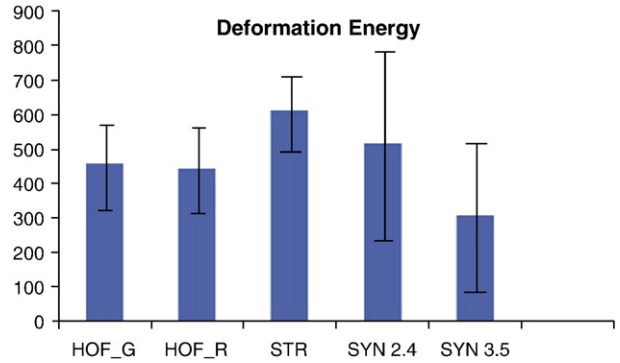

Fig. 9. Deformation energy: this lists the energy which was stored in the system until failure. This energy has parts of elastic and plastic deformation. The black bars show the standard deviation of the mean value which is depicted through the light grey bars.

As can be seen, the different implants clearly act differently in the load to failure scenario. The implants with higher screw-count of the distal fracture system like Hofer®, Synthes® 2.4 or Stryker® (5 screws) lead to higher ultimate forces than the implant with just 3 screws (Synthes® 3.5). It is interesting that there is practically no difference in ultimate force and fracture energy between the two variations of the Hofer® implant with corticalis and spongiosa locking screws.

5. Discussion

To allow an interpretation of the properties of the examined implants, the applied process of bone-healing has to be understood [16–18,22]. In the case of distal radius fractures, the most important process of healing is the secondary fracture healing [5]. Small relative movements of the fracture fragments cause the formation of a so called Callus. The Callus assists in the healing process [7]. However, the fragments should not move to loose, because this increases the risk of healing with a deviation of the right angle which can result in reduction of mobility. An upper limit for the targeted stiffness of the fracture is at the moment unknown [8,9,14]. What is relatively well established is the value of fracture strain. This fracture strain expresses the elastic change of fracture width divided by the absolute width of the fracture in unloaded condition. According to a study by Perren [21] the value of fracture strain of 0.3 leads to most beneficial results if indirect (=secondary) fracture healing is applicable as in our case.

It is important to emphasize the difference between fracture strain, which is dependent on elastic deformation, and the effects of permanent deformation. Even if a certain (not minimal) elastic deformation is beneficial, permanent deformation doesn't assist in the formation of a callus, but leads to permanent deviations of the anatomically correct position of the fragments after healing. The primary focus when using radius implants should therefore be the minimization of permanent deformations during the healing phase of four to six weeks after implantation [e.g. 4]. Every movement of the body part loads the system of implant and bone which successively increases the damage which leads to permanent deformations. The elastic movement of the bone is determined by the stiffness of the system, but doesn't lead to permanent tilts of the system. Therefore, the optimization of stiffness should be credited only second priority.

5.1. Discussion of stabilization of the sagittal fracture gap under fatigue

The implants show different axial stiffness. The axial stiffness has different components: The proximal and distal fracture system have the greatest influence on the stiffness of the system. Furthermore, the stiffness of the implant itself and of the surrounding bone material has effects. The load to failure analysis shows that the ultimate force for failure of the distal part of the implant (tranversal fracture system) is about 2000 N, about 3 times higher than the maximum force of the fatigue period. (note, the load to failure experiment was carried out on samples after they were fatigue tested). Due to the higher count of screws, the load on one single distal screw is lower than the load on the proximal screws (with the exception of the SYN_3.5 implant).The load is distributed to more screws (instead for the SYN_3.5 implant), resulting in high stiffness. Therefore the system is likely to stay elastic during the fatigue sequence and fatigue effects will be more profound on the proximal side. The effect of implant stiffness is also not likely to change during the fatigue sequence and no fatigue is expected for the implant plate. The bone material far from load insertion points (like screw holes, etc.…) is also not expected to change drastically during the experiment.

As a result, the changes in axial stiffness can be mainly attributed to effects of the two proximal screws transferring load from the implants to the proximal bone shaft. As can be seen in Fig. 4, the axial stiffness shows an increase for small cycle counts. This effect was also experienced at fatigue testing of implanted tibia bones [10]. It can be explained through two effects: Local hardening of the bone material and an initial period of "fitting" when the screws are arranged on sub mm scale in positions leading to highest stiffness. This fitting period is also present after implantation of real bones and therefore still allows the comparison of different implants. The effect of local hardening is suspected to be much smaller than the effect of the fitting period. It should be present during the whole fatigue experiment and results in a small increase in stiffness. It can be seen in the case of the HOF_R implant where other effects like screw or bone fatigue failure is low. Local hardening occurs, because the load is always positive and the resistance of the bone material is, to a certain extent before breaking occurs, proportional to the compressive deformation (which increases with higher cycles as shown in Fig. 5). As a result, the stiffness of the bone material increases due to fatigue which explains the slow-down of the increase of axial permanent deformation at higher cycles (Fig. 5). Since the stiffness of the implant is much higher than the stiffness of the supporting bone, changes of implant properties due to fatigue are for the most cases negligible. It is however possible, that a drastic change of specimen alignment as recorded for the Stryker implant (see below), leads to higher lever arms and therefore locally very high peak loads on special parts of the implant (like the head of the most proximal screw). These parts can get into the plastic regime even though their stiffness is much higher than the bone material and also show fatigue damage.

The second very important parameter for discussion of implant quality is the permanent deformation. The permanent deformation can be correlated with the permanent tilting angle of the implant. The tilting angle allows making direct conclusions about the anatomical functionality of the implanted bone (see Section 3).

The SYN_3.5 implant shows the lowest stiffness which can be due to the fact, that the distal screws are positioned further from the sagittal fracture than in case of the other implants (see Fig. 1), thus leading to higher lever arm on the screws which promotes fatigue phenomena. Moreover, due to the sagittal fracture, only two distal screws can practically transfer loads from the bone to the implant therefore the assembly of implant and screws is not as rigid as for implants incorporating more screws on the distal side. Due to the relatively higher loads on all screws, fatigue damage, expressed in terms of permanent deformation is the second highest for all tested implants. The permanent tilting angle is about 3° after 2000 loading cycles which is below the margin for implant failure (5°).

The SYN_2.4 implant incorporates 5 locking screws on the distal side of the transversal fracture gap and 2 locking screws to fix the implant to the proximal bone shaft. The results of axial stiffness and permanent deformation show a higher axial stiffness and less than halved axial deformation. In our scenario, the implementation of locking screws and the increased number of screws lead to better results for this implant when compared to SYN_3.5.

The implant produced by Stryker® showed a very unstable evolution of stiffness and a very high permanent deformation. During the fatigue loading, the screw-hole of the most proximal screw widened and the proximal screw moved more proximal. This leads to a reduction of the fracture gap, high permanent deformation/tilting angle and high damage to the head of the screw (see Fig. 9). The reason for the high loading of the most proximal screw is the high lever arm. Even though two screws on the proximal side are used to fix the implant to the bone shaft, they are positioned next to each other. Under loading, the friction forces are reduced since two screws cannot fix the implant to the synthetic bone and most of the load is transferred directly through the screws. This leads to high stresses at the screw heads, especially if the screws come loose because of fatigue damage. Examination of the damage showed that the head of the most proximal screw was damaged as a result of fatigue. The permanent deformation of this implant is more than twice the permanent deformation of any other implant. The corresponding permanent tilting angle is more than 6°, an obvious indication of implant failure.

The Hofer® implant was tested using two different implementations of the distal screws (see Section 1). The two variations lead to different fatigue behaviour. If all distal screws are implemented as corticalis-locking screws, the implant shows the highest stiffness and lowest permanent deformation of all examined implants. If the distal row of screws is substituted with spongiosa locking screws, the implant properties deteriorate. The greatest effect was measured for the permanent tilting angle. The substitution of corticalis-locking screws with spongiosa locking screws leads to an increase of tilting angle from 1.4° to 2.6°.

5.2. Stabilization of the sagittal fracture gap

The stabilization of the sagittal fracture gap was characterized analogously to the transversal fracture gap using the parameters' stiffness and permanent deformation.

The stiffness of the sagittal fracture gap is about one order of magnitude higher than the axial stiffness. Most implants show a nearly constant stiffness, with exceptions of the Synthes® 3.5 and Hofer® implants using corticalis and spongiosa screws (HOFER_G). Synthes® 3.5 shows a successive decrease of stiffness during the first 600 cycles; afterwards the stiffness stabilizes at about 4300 N/mm. This can be due to the fact that the middle-screw of the distal segment looses contact with the bone since it is positioned in the fracture gap. The HOFER_G implant provides the lowest stiffness at the end of the fatigue sequence, even if the initial stiffness measured during the first loading cycles was the same as in the case of the HOFER_R implant where corticalis-locking screws were used on the distal side. It is noticeable also in this area, that the incorporation of corticalis-locking screws is beneficial.

The permanent deformation of the sagittal fracture gap is very low. The maximum value of 0.14 mm is reached by the Stryker® implant, followed by the HOFER_G implant. However, the absolute value is so low, that it is negligible from a medical point of view. It is interesting, that the difference between the HOFER_G and HOFER_R is noticeable; the HOFER_R implant leads to relatively lower permanent deformation of the sagittal fracture gap.

As described above, failures during the fatigue loading occurred mainly proximal of the transversal fracture gap. To test the fixation of the sagittal fracture gap and simulate possible failure modes, a load to failure test was carried out. It showed that most implants withstand high load of up to 2500 N even after 2000 cycles of fatigue testing. The implant SYN_3.5 shows the lowest ultimate force of about 1300 N. The comparison with implant SYN_2.4 is interesting. Both plates have relatively similar geometry (similar lever arms) but incorporate different type and number of screws: The SYN_2.4 implant uses 5 locking screws of smaller diameter; the SYN_3.5 uses 3 screws of larger diameter. The results show, that the variant with more screws of smaller diameter leads to higher ultimate force and increased deformation energy. The major disadvantage of the variant with only three screws on the distal side is that one of the screws is positioned directly in the fracture gap, therefore reducing the effective number of load-transferring screws to two.

HOF_G and HOF_R implants lead to the same results, further study of the breaking shows that not the bone material, but the gears of the proximal locking screws in the implant plate fail, the fixation of the distal part is sufficient in both cases.

6. Restrictions of this study

The reason for using a synthetic bone is based on the advantages of easy handling and the small spread of mechanical properties of these standardized bones. It is important to emphasize the comparative character of this study. The used bones need to be evaluated for their suitability in mechanical tests. Moreover, a real bone is a dynamic object and the effects of the bone-healing process cannot be incorporated in an anatomical model. Furthermore, heating of tissue during implantation and the loading cycles could cause necrosis of osteonal tissue surrounding the implant and changing the properties of the system. Since the healing process is likely to improve the properties of the system (with respect to fixation), we expect our values to be conservative. Nevertheless, to verify this thesis, further studies like [24] comparing the material properties of synthetic bones and real human bones are needed. Therefore, the direct application of our results is not allowed. Nevertheless, the use of synthetic bones is legitimate because even if the absolute values may differ from the clinical ones, differences between the various nailtypes are noticeable.

Physiological conditions (saline solution) have not been considered in this study, and will be investigated in another work to characterize its influence on the fatigue properties of the system.

The testing setup allows getting only limited information about the movement and condition of individual objects like screw and implant. The whole system is evaluated and the sum of all effects is measured which needs careful preparation of the results. However, the effort to measure the position of every part of the system would be very high, and would most likely lead to problems with the deduction of realistic data from the experiment (like for instance the needed mechanical installations). We therefore concentrated on the whole system and deducted medically relevant data through the characterization of implant quality with permanent deformation and tilting angle.

7. Conclusion

The results from the fatigue experiments lead to the following conclusions.

The proximal fixation of the implant to the bone shaft is more critical than the distal load transfer. The worst results were associated with high lever arms and too few load-transferring screws on the proximal side of the sagittal fracture.

The implants providing best fatigue resistance are HOFER and SYNTHES_2.4. This is due to the combination of relative small lever arms, stable fixation of the distal fragments and fatigue resistant screws. The implant SYNTHES_3.5 showed drawbacks because of the low number of screws on the distal side. The behaviour of the Stryker implant could be improved by inserting an additional screw in the elongated hole, even if this screw would not transfer axial loads, it would prevent the implant from detaching and therefore increase load transfer through friction between bone and implant-plate. Moreover, the screws of this implant showed low fatigue strength (damage to the heads).

Generally, it is beneficiary to use an additional screw at the most distal position proximal of the fracture gap possible. This would reduce the load on the other screws and lower permanent deformation and higher stiffness are expected.

The use of corticalis-locking screws leads to better results for both the sagittal and transversal fracture system and should be preferred if possible.

Acknowledgements

The authors thank Ing. Karl Kropik for the preparation of the samples, as well as Mrs. Prof. Stanzl-Tschegg, Mr. MD Weninger and Mr. Dipl.-Ing. Jamek for their contribution to the scientific discussion.

References

[1] C. Kanchanomai, V. Phiphobmongkol, P. Muanjan, Eng. Fail. Anal. 15 (2008) 521.
[2] C. Gaebler, S. Stanzl-Tschegg, G. Heinze, B. Holper, T. Milne, G. Berger, V. Vecsei, Fatigue strength of locking screws and prototypes used in small diameter tibial nails, vol. 47, 1999, p. 379.
[3] C. Fleck, D. Eifler, Adv. Eng. Mater. 9 (12) (2007) 1069.
[4] H. Drobetz, A.L. Bryant, T. Pokorny, R. Spitaler, M. Leixnering, J.B. Jupiter, Volar fixedangle plating of distal radius extension fractures: influence of plate position on

secondary loss of reduction — a biomechanic study in a cadaveric model, J. Hand Surg. Am. 31 (12) (2006) 615.
[5] E.K. Tschegg, S. Herndler, P. Weninger, M. Jamek, S. Stanzl-Tschegg, H. Redl, Stiffness Analysis of Tibia-Implant System under Cyclic Loading, Materials Science and Engineering C 28 (2008) 1203.
[6] Weninger P, private communication, Sept. 2007.
[7] I. Youn, J.K.F. Suh, G.D. Jones, Orthopaed. Res. Soc. Abst. 29 (2004) 134.
[8] D.R. Epari, H. Shell, S. Muchow, et al., Orthopaed. Res. Soc. Abst. 29 (2004) 251.
[9] R. Schmidhammer, S. Zandieh, R. Mitermayr, L.E. Pelinka, M. Leixnering, M. Hopf, A. Kroepfl, H. Redl, J. Trauma Inj. Infect. Crit. Care 61 (2006) 199.
[10] Schüller M, Herndler S, Weninger P, Jamek M, Redl H, Tschegg E K;Stiffness and permanent deformation of extra-articular distal Tibia fractures treated with unreamed small diameter intramedullary nailing. Materials Science and Eng. C 28 (2008) 1209.
[11] Melanie Kebernik, (2005) Charakterisierung der mechanischen Eigenschaften der Schrauben-Knochen-Verbindung im kortikalen Knochen, Dissertation an Universität Ulm, Medizinische Fakultät, Institut für Unfallchirurgische Forschung und Biomechanik, 2005.
[12] A.M. Weinberg, C. Castellani, M. Arzdorf, E. Schneider, B. Gasser, B. Linke, Clin. Biomech. 22 (2007) 502.
[13] J. Korner, G. Diederichs, M. Arzdorf, H. Lill, Ch. Josten, E. Schneider, B. Linke, J. Orthop. Trauma 18 (5) (May/June 2004) 286.
[14] R.B. Salter, D.F. Simmonds, B.W. Malcolm, E.J. Rumble, D. MacMichael, N.D. Clements, J. Bone Jt. Surg. Am. 62 (1980) 1232.
[15] D. Osada, S.F. Viegas, M.A. Shah, R.P. Morris, R.M. Patterson, J. Hand Surg. Am. 28 (2003) 94.
[16] J.D. Tavakolian, J.B. Jupiter, Dorsal plating for distal radius fractures, Hand Clin. 21 (2005) 341.
[17] R. Grewal, B. Perey, M. Wilmink, K. Stothers, J. Hand Surg. Am. 30 (2005) 764.
[18] D. Ring, K. Prommersberger, J.B. Jupiter, J. Bone Jt. Surg. Am. 87 (Suppl 1) (2005) 195.
[19] A.A. Willis, K. Kutsumi, M.E. Zobitz, W.P. Cooney III, J. Bone Jt. Surg. Am. 88 (2006) 2411.
[20] M. Blythe, K. Stoffel, P. Jarrett, M. Kuster, J. Hand Surg. Am. 31 (2006) 1587.
[21] S.M. Perren, J. Bone Jt. Surg. 84-B (8) (November 2002) 1093.
[22] K.-P. Schmit-Neuerburg, H. Towfigh, R. Letsch, (Hrsg.), Tscherne Unfallchirurgie, Teil1, Springerverlag, 2001.
[23] Injections-Mörtel FIS VS 100 P der Firma Artur Fischer GmbH, 2009.
[24] F. Liska, S. Eichhorn, U. Schreiber, R. Burgkart, R. Gradinger, Vergleich der mechanischen Eigenschaften von spongiösen Knochen verschiedener Spezies und künstlicher Knochen (Comparison of mechanical properties of spongious bones of different species and synthetic bones), German Medical Science GMS Publishing House, 2008 Doc WI74-1071.